Journal of Nuclear Medicine, published on July 22, 2021 as doi:10.2967/jnumed.121.261926

*Original article*

# First-in-human study of $^{89}$Zr-pembrolizumab PET/CT in patients with advanced stage non-small-cell lung cancer

RUNNING TITLE

$^{89}$Zr-pembrolizumab in NSCLC patients

Anna-Larissa N Niemeijer[1], Daniela E Oprea-Lager[2], Marc C Huisman[2], Otto S Hoekstra[2], Ronald Boellaard[2], Berlinda J de Wit-van der Veen[3], Idris Bahce[1], Daniëlle J Vugts[2], Guus AMS van Dongen[2], Erik Thunnissen[4], Egbert F Smit[1,5], Adrianus J de Langen[1,5]

[1]Department of Pulmonary Diseases, Cancer Center Amsterdam, Amsterdam University Medical Centers (location VU University Medical Center), Amsterdam, the Netherlands

[2]Department of Radiology & Nuclear Medicine, Cancer Center Amsterdam, Amsterdam University Medical Centers (location VU University Medical Center), Amsterdam, the Netherlands

[3]Department of Nuclear Medicine, NKI-AvL, Amsterdam, the Netherlands

[4]Department of Pathology, Cancer Center Amsterdam, Amsterdam University Medical Centers (location VU University Medical Center), Amsterdam, the Netherlands

[5]Department of Thoracic Oncology, NKI-AvL, Amsterdam, the Netherlands

Disclosures

All authors declare no conflict of interest.

Correspondence:

Adrianus J. de Langen, MD, PhD

Department of Thoracic Oncology

NKI-AvL

Plesmanlaan 121

1066 CX Amsterdam

The Netherlands

Telephone number +31 20 5129111

Email: j.d.langen@nki.nl

First author

Anna-Larissa Niemeijer (PhD-student, resident Pulmonary Diseases)

Amsterdam UMC

Department of Pulmonary Diseases

De Boelelaan 1118

1081 HV Amsterdam

The Netherlands

Telephone number +31 20 4444782

Email:an.niemeijer@amsterdamumc.nl

Word count: 4960

Financial support

We received a research grant for the implementation of this study from Merck Sharpe & Dohme (MSD). MSD was not involved in the study design, nor in the data collection, analysis and interpretation of data, nor in the writing of this report.

**Abstract**

**Background**

Tumor programmed-death ligand-1 (PD-L1) proportion score is the current method to select non-small-cell lung cancer (NSCLC) patients for single agent treatment with pembrolizumab, a programmed cell death-1 (PD-1) monoclonal antibody. However, not all patients respond to therapy. Better understanding of *in vivo* drug behavior may help to select patients that benefit most.

**Methods**

NSCLC patients eligible for pembrolizumab monotherapy as first or later line therapy were enrolled. Patients received two injections of $^{89}$Zr-pembrolizumab; one without a preceding dose of pembrolizumab and one with 200 mg pembrolizumab, directly prior to tracer injection. Up to four PET/CT scans were obtained after tracer injection. Post-imaging acquisition, patients were treated with 200 mg pembrolizumab, every three weeks. Tumor uptake and tracer biodistribution were visually assessed and quantified as standardized uptake value (SUV). Tumor tracer uptake was correlated with PD-1 and PD-L1 expression and response to pembrolizumab treatment.

**Results**

Twelve NSCLC patients were included. One patient experienced grade 3 myalgia after tracer injection. $^{89}$Zr-pembrolizumab was observed in the blood pool, liver and spleen. Tracer uptake was visualized in 47,2% of 72 tumor lesions measuring ≥20 mm long axis diameter, and substantial uptake heterogeneity was observed within and between patients. Uptake was higher in patients with response to pembrolizumab treatment (n=3) compared to patients

without a response (n=9), although this was not statistically significant (median SUVpeak 11.4 vs 5.7, p=0.066). No significant correlations were found with PD-L1 or PD-1 immunohistochemistry.

**Conclusions**

$^{89}$Zr-pembrolizumab injection was safe with only one grade 3 adverse event, possibly immune related, out of 12 patients. $^{89}$Zr-pembrolizumab tumor uptake was higher in patients with response to pembrolizumab treatment, but did not correlate with PD-L1 or PD-1 immunohistochemistry.

Count: 275 words (max 350 words)

Keywords: NSCLC, immunotherapy, PET-imaging

## Introduction

Immune checkpoint inhibitors have changed the treatment paradigm of advanced non-small-cell lung cancer (NSCLC). However, identifying individual patients who benefit from immune checkpoint inbitors remains challenging. Better selection of patients will likely lead to higher response rates, less unnecessary toxicities and reduced costs. The current method of selecting patients for treatment with single agent pembrolizumab, a programmed cell death-1 (PD-1) monoclonal antibody, consists of scoring tumor programmed death ligand 1 (PD-L1) expression using immunohistochemistry. Although pembrolizumab monotherapy has been approved for the first and second line treatment of NSCLC patients with a PD-L1 tumor proportion score (TPS) of 1% and greater, only 28% of patients show a response to treatment, according to RECIST 1.1, with the highest response rate being 40-45% for patients with a TPS of ≥50% (*1-4*). At the same time ~10% of patients without tumor PD-L1 expression respond to treatment (*1,5*).

Positron Emission Tomography (PET) with radiolabeled antibodies visualizes and quantifies pharmacokinetics in vivo, which may help understanding antibody behavior in blood and tissues (*6*). Previous research in NSCLC patients with radiolabeled immune checkpoint inhibitors revealed intra- and interpatient heterogeneity of tumor uptake for $^{89}$Zr-nivolumab (PD-1) and $^{89}$Zr-atezolizumab (PD-L1) (*7,8*). $^{89}$Zr-atezolizumab uptake strongly correlated with response, whereas $^{89}$Zr-nivolumab uptake correlated with lesional response, but not overall response. Studies in humans with $^{89}$Zr-labeled pembrolizumab have not been performed yet. Preclinical studies with $^{64}$Cu- and $^{89}$Zr-labeled pembrolizumab in mice and rats reported uptake in spleen and liver and specific targeting of PD-1 (*9,10*). Although nivolumab and pembrolizumab are PD-1 blocking antibodies with structural similarities, the binding surface to PD-1 differs (*11-13*). In

this feasibility study, we aimed (i) to investigate whether administration of $^{89}$Zr-pembrolizumab is safe, (ii) to assess the biodistribution of $^{89}$Zr-pembrolizumab and (iii) to correlate the tracer uptake with PD-1 and PD-L1 immunohistochemistry and response to pembrolizumab treatment.

## Materials and methods

*Patients*

The study was conducted according to the Declaration of Helsinki. The institutional review board (Medical Ethics Committee of the Amsterdam UMC, location VU University Medical Centre, Amsterdam) approved this study and all subjects signed a written informed consent. The trial was registered at www.clinicaltrials.gov (Clinical Trials Identifier: NCT03065764). Twelve patients with advanced NSCLC eligible for pembrolizumab treatment were included in this multicenter trial.

*Tumor biopsies*

Histological tumor biopsies were obtained before the first $^{89}$Zr-pembrolizumab injection and after the last line of systemic therapy, in case patients received prior therapy. Tumor tissue sections were stained with hematoxylin and eosin (H&E), PD-L1 (Dako's PD-L1 IHC 22C3 pharmDx) and PD-1 (Cell Marque Corporation Clone NAT105 antibody). An experienced thoracic pathologist (E.T.), blinded for clinical information, evaluated the slides. PD-L1 and PD-1 expression were measured as total (both tumor and immune cells) PD-L1 and PD-1 expression. In addition, tumor PD-L1 expression was scored as the percentage of tumor cells showing positive staining in the sample. PD-L1 was scored according to the 22C3 scoring guidelines (*14*).

PD-L1 and PD-1 were also scored according to the SP142 scoring system (IC0, IC1, IC2 to IC3) (*15*), but still with the 22C3 antibody.

*$^{89}$Zr-pembrolizumab*

$^{89}$Zr-pembrolizumab was produced in compliance with current Good Manufacturing Practice at Amsterdam UMC, location VU according to validated procedures (*16-18*). Pembrolizumab was labeled with $^{89}$Zr in an inert way to ensure that $^{89}$Zr-pembrolizumab kinetics fully resemble kinetics of unlabeled pembrolizumab (*19,20*). $^{89}$Zr-pembrolizumab was produced as previously described with slight modifications (*19*). A detailed description of the production process is described in the Supplemental material.

*Study design*

The study protocol consisted of two imaging series per patient, one without and one with a predose of unlabeled pembrolizumab, respectively (Supplementary figure 1). $^{89}$Zr-pembrolizumab (37 MBq ±10%, 2 mg pembrolizumab) was intravenously (IV) injected on day 0. Static whole body PET/CT scans from skull vertex to mid-thighs were performed 1h, and 3, 5 and 7 days post injection (p.i.) for the first 3 patients, while all other patients were scanned on day 3 and 6 p.i. On day 12, patients received an infusion with 200 mg unlabeled pembrolizumab, within two hours followed by a second $^{89}$Zr-pembrolizumab injection, to maximize the chance of representing therapeutic tumor targeting. Diagnostic CT scan of thorax and upper abdomen and a brain MRI were obtained prior to the start of treatment. Pembrolizumab (200 mg flat dose) was administered every 3 weeks until disease progression, unacceptable toxicity or withdrawal

of consent. Response assessment was performed with diagnostic contrast-enhanced CT scan of thorax and upper abdomen +/- brain MRI (latter only in case of pretreatment brain metastases) every 9 weeks during treatment or more frequently if clinically indicated and assessed according to RECIST 1.1 (*21*). Durable clinical benefit (DCB) was defined as partial response (PR) or stable disease (SD) ≥6 months.

*PET acquisitions*

PET acquisitions were performed using an EARL calibrated Philips Ingenuity TF, Philips Big Bore or Philips TF TOF PET/CT scanner (Philips Healthcare®, the Netherlands/USA), at 10 minutes/bed position over the area containing the primary tumor, and 5 minutes over the remaining bed positions. Following this PET, a low dose CT (50 mAs, 120 kV) was acquired for anatomical correlation and attenuation correction. Whole body data were corrected for dead time, decay, scatter and randoms, and reconstructed with a matrix size of 144x144 and voxels of 4x4x4 $mm^3$, using a time of flight iterative reconstruction method (BLOB-OS-TF). The transaxial spatial resolution was ~5 mm full width at half maximum in the center of the field of view.

*PET/CT analyses*

Reconstructed images were transferred to off-line workstations for further analysis. Tumor accumulation was assessed by an experienced nuclear physician (D.O.) and described as focal or diffuse uptake exceeding the local background and incompatible with physiological uptake. Volumes of interest (VOIs) were manually delineated on each scan using the Accurate tool (*22*). Liver, spleen, brain, lungs and kidneys were manually delineated on each scan using the low-dose CT as anatomical reference (*23*). Fixed VOIs were placed in the descending aorta to

measure blood pool activity and in the lumbar vertebrae to estimate the bone marrow activity concentration. Tracer uptake in all delineated VOIs was quantified semi-quantitatively as standardized uptake value (SUV). From each VOI, we derived the mean and peak activity concentrations (Bq/cc), normalized for body weight. SUVmean is reported for organ tracer uptake and SUVpeak for tumor lesions (*24*). To compare tracer uptake between imaging series 1 and 2, the percentage injected dose per gram tissue (%ID/gr) was calculated. To avoid partial volume effects, only results of tumor lesions exceeding 20 mm long axis diameter are reported.

*Blood samples*

Blood samples for $^{89}$Zr-pembrolizumab concentration were obtained at 5, 30, 60 and 120 minutes p.i. for the first 3 patients. For the other patients, blood samples were drawn at 5 and 30 minutes p.i.. Plasma and whole blood concentrations were assessed by radioactivity measurements in a cross-calibrated γ-counter (Wallac Wizard 1480; PerkinElmer Inc.). Plasma activity concentration was calculated as %ID/gr.

*Adverse events*

Adverse events were recorded from initial signing of the informed consent to the second full dose of pembrolizumab. The National Cancer Institute Common Terminology Criteria for Adverse Events version 4.0 were used (*25*).

*Statistical analysis*

Statistical analysis were performed using SPSS statistics for Windows Version 26.0. Median SUVpeak of all delineated lesions (long axis diameter ≥20 mm) per patient was calculated and used to compare the median value between patients with DCB and without DCB. Because of the low patient number, PD-1 immunohistochemistry was dichotomized as “PD-1 low” (IC0 and IC1) and “PD-1 high” (IC2 and IC3). Mann-Whitney-Wilcoxon rank sum test was performed to evaluate differences in SUV in response and immunohistochemistry. Progression-free survival (PFS) was summarized using Kaplan-Meier plots. PFS was defined from the date the patient received the first pembrolizumab cycle to the date of radiological progression or death (whichever occurred first). Median SUVpeak of the full cohort was used to stratify high vs low uptake, and Log-rank to compare both groups. Correlation between SUVpeak of tumor lesions on different scan days was calculated using the Spearman’s rank correlation coefficient. Wilcoxon signed rank test and Friedman test were performed for paired data (multiple groups). P-values less than 0.05 were considered to be statistically significant.

## Results

### *Patients*

Twelve patients, 5 chemotherapy naive and 7 with progression after first or second line treatment, were enrolled (Supplementary Table 1). All patients had histopathologically confirmed lung adenocarcinoma. Patients who were chemotherapy-naive had higher PD-1 and PD-L1 expression rates compared to patients that received prior chemotherapy. Eight patients completed the full imaging series. In patient 2 and 3, the scan at day 12 respectively day 14 was not performed due to logistical problems. Patient 6 did not receive the second injection nor

treatment because of a large brain metastasis that required immediate treatment and patient 7 refused to undergo the last PET/CT scan because of dyspnea. In patient 12 only a scan of the thorax could be obtained at day 6, 15 and 18, because of severe myalgia (grade III).

*Safety*

The most frequently reported adverse events were fatigue, anorexia and dyspnea (Supplementary table 2), most of which were disease related. In one patient grade III anemia was observed, but the onset was prior to tracer injection. One patient experienced grade III myalgia after the first $^{89}$Zr-pembrolizumab injection. This patient discontinued treatment after the first pembrolizumab cycle because of the myalgia and had progressive disease within 6 months after start of treatment.

*Pharmacokinetics*

To explore whether micro dosing of the tracer (2 mg) can be used to image tumor uptake, we compared %ID/gr in plasma, in organs and in tumor lesions between the first and the second imaging acquisition. Plasma clearance was slower for imaging acquisition part 2 compared to part 1 (Supplementary Figure 2). Because of limited data, no statistical tests were performed. The concentration of pembrolizumab in the spleen was lower in part 2, suggesting that the spleen serves as 'sink' (Supplementary Figure 3).

For the other organs no differences were observed in %ID/gr between imaging acquisition part 1 and part 2 for the first three patients (Supplementary Figure 2). Remarkably, not all tumor lesions that were identified in part 1 could be assessed in part 2 (Supplementary table 3).

Nineteen tumor lesions could be identified in 10 patients on multiple time points in part 1 and 10 lesions were visible on multiple time points in part 2 (Supplementary Figure 3). In two patients, %ID/gr in the primary tumor was higher in part 2 compared to part 1 (Supplementary Figure 3). In the next paragraphs, only data of acquisition part 1 are shown.

*Biodistribution of $^{89}$Zr-pembrolizumab*

On the first PET/CT scan (performed 1h p.i.), $^{89}$Zr-pembrolizumab uptake was observed in the blood pool, liver, spleen and kidneys (Figure 1A). In 2 out of 3 patients (66.6%) also the gallbladder was visualized (Figure 1A). Circulating $^{89}$Zr-pembrolizumab in the blood pool was highest (SUVmean 11.5±1.4 1h p.i.) at 1h p.i. and decreased over time (SUVmean 4.6±1.2, 3.0±0.5 and 2.3±0.6 on day 3, 5 and 7 p.i. respectively, Figures 1A-B). Uptake was high in liver and spleen (SUVmean 3.9±1.4 and 5.5±1.4, respectively, on day 3 p.i., Figure 1A-B) and this remained stable over day time (liver: SUVmean 4.1±1.6 on day 5 p.i. and 4.0±1.6 on day 7 p.i and spleen: SUVmean 5.4±1.4 on day 5 p.i. and 5.6±1.2 on day 7 p.i.). Intestinal uptake was variable (Figure 1A), and low uptake was seen in kidneys, bone marrow, non-tumor bearing lung tissue and brain (on day 3 SUVmean 3.0±0.6, 2.4±0.5, 1.3±0.7 and 0.4±0.1, respectively). In 8 out of 12 patients, non-malignant lymph nodes and/or adrenal glands showed low tracer uptake (examples are shown in Supplementary Figure 4). In patient 1, an axillary lymph node (not suspected for malignancy on the $^{18}$F-FDG PET/CT scan) that showed low tracer uptake was biopsied. Histopathological examination showed a high density of PD-1 positive lymphocytes in the secondary lymphoid follicles and no malignant cells. The adrenal glands of patient 3 were

slightly enlarged at baseline, but not suspected for metastases based on the $^{18}$F-FDG PET/CT scan, and the adrenal glands remained unchanged during follow-up CT scans.

*Tumor uptake*

Overall, a total of 216 lesions from 12 patients were delineated on the pretreatment diagnostic CT scan (Table 1). Of these lesions, 140 (64.8%) had a diameter <20 mm, 4 lesions were difficult to measure due to atelectasis and 72 (33%) had a diameter ≥20 mm. Sixty-two lesions (28.7%) were visible on PET/CT. Of the lesions with a diameter less than 20 mm, 26 lesions out of 140 (18.6%) were visible on PET/CT on day 6 or 7. Of the lesions with a long axis diameter ≥20 mm, 34 out of 72 (47.2%) were visible. Two lesions were difficult to measure. In all patients, at least one malignant lesion showed tracer uptake (median 4.5, range 2-17 per patient). For the first 3 patients, median SUVpeak of tumor lesions increased in time from 4.9 [IQR 3.5-6.6] on day 3 to 5.2 [IQR 4.0-6.8] on day 5 to 5.9 [IQR 4.0-7.0] on day 7 p.i. (Figure 2). There was no significant increase between day 5 and 7 p.i. (p=0.28). Intralesional tracer distribution was heterogeneous (Figure 3) and uptake patterns were variable (Figure 4 A-D).

Four patients had brain metastases (38 lesions in total), of whom three had been treated with (stereotactic) radiotherapy before start of this study (18 out of 38 lesions) (Supplementary table 4). Increased tracer uptake was observed in 2 patients (3 metastases): one patient received whole brain radiotherapy 9 months prior to PET-imaging (1 visible brain metastasis, long axis diameter 33.1 mm, Figure 4D) and 1 patient had not been irradiated before (2 visible brain metastases, long axis diameter 31.9 and 19.3 mm).

*Response*

For response evaluation, we report SUVpeak on day 6 or 7 because tumor uptake was the highest and blood pool activity the lowest, thus offering the best tumor-to-background ratio. Three patients had DCB to pembrolizumab: 1 had PR according to RECIST 1.1 and 2 had SD. Patients with DCB had a higher median tracer uptake, but this was not significant (median SUVpeak 11.4 vs 5.7, p=0.066, Figure 5A). $^{89}$Zr-pembrolizumab uptake increased with best response category according to RECIST 1.1 (p=0.047, Figure 5B). No partial response was observed in the PET negative lesions. Patients with a SUVpeak higher than the median (SUVpeak 6.7) had longer PFS (median PFS 25.0 weeks) compared to those with a SUVpeak lower than the median (median PFS 7.0 weeks), although this was not significant (p=0.21) (Figure 5C).

*Immunohistochemistry*

Not all biopsied lesions (n= 7/12) showed $^{89}$Zr-pembrolizumab uptake (Supplementary table 5). PD-1 expression and tracer uptake were not correlated (median SUVpeak 7.9 for patients with high PD-1 expression vs 7.4 for patients with low expression, p=1.0), as well as PD-L1 expression and tracer uptake (median SUVpeak 7.6 for patients with TPS <49% and median SUVpeak 7.4 for patients with TPS ≥50%, p=0.72) (Figure 6AB). Pre-treatment PD-1 expression did not correlate with response (p=0.41), whereas pretreatment PD-L1 expression ≥50% did predict for response (p=0.049).

**Discussion**

This first-in-human study of $^{89}$Zr-pembrolizumab shows that injection of $^{89}$Zr-pembrolizumab was well tolerated, with one possibly related adverse event. Tumor lesions could be visualized and quantified. For all patients, at least one tumor lesion showed tracer uptake after a single $^{89}$Zr-pembrolizumab injection. Tumor uptake was heterogeneous within and between patients, and only 47.2% of the lesions with a long axis diameter ≥20 mm showed uptake on the $^{89}$Zr-pembrolizumab PET/CT scan.

All patients (except patient 6) underwent two imaging acquisitions, one without a predose of unlabeled pembrolizumab and one with a predose. Plasma clearance was slower when predose was used. We observed lower tracer uptake in spleen in part 2 compared to part 1, which suggest that the predose saturated the PD-1 receptors in the spleen. In part 2 (with co-injection of a predose), only 10 lesions could be delineated in the first three patients, while 19 lesions could be delineated in these patients in part 1. We assume that a predose of 200 mg (flat dose of pembrolizumab) occupies most available PD-1 receptors causing loss of signal. Recently, a flow cytometry study in patients treated with pembrolizumab showed receptor occupancy on peripheral mononuclear blood cells at the end of first infusion between 88-100% depending on cell type (*26*). Unfortunately, because of our limited data we cannot determine an 'optimal predose' of unlabeled pembrolizumab.

Biodistribution of $^{89}$Zr-pembrolizumab was comparable to that observed in previous NSCLC studies with $^{89}$Zr labeled immune checkpoint inhibitors. High uptake was seen in the liver (likely due to tracer catabolism), the spleen (likely due to binding to PD-1 receptors on lymphocytes and dendritic cells, abundantly present in the spleen) and non-malignant lymph nodes (*7,8*). PD-1 is expressed on a variety of immune cells, including activated and exhausted CD8$^{+}$ T cells, B

cells, myeloid dendritic cells and monocytes, and in fact most patients showed $^{89}$Zr-pembrolizumab uptake in non-malignant lymph nodes (*27*). Recent preclinical imaging studies with $^{89}$Zr-pembrolizumab in mice and monkeys also reported high uptake in lymphoid tissues (*28,29*). Variable uptake was observed in the intestines, probably due to excretion. In none of the patients included in this study, colitis was observed during pembrolizumab treatment. Low uptake was observed in the kidneys, adrenal glands, bone marrow, lungs and central nervous system, suggesting that this tracer has a beneficial profile for imaging lung cancer patients. In this study, we observed tracer uptake in some brain metastases. Since the majority of brain metastases were pretreated with radiotherapy and small in size (less than 20 mm), these factors could have contributed to absence of tracer accumulation in a number of these lesions.

Tracer uptake in non-malignant lymph nodes is regarded as specific uptake. Lymph nodes are known for their role in the immune defense to pathogens and tumor draining lymph nodes are needed to engage an optimal antitumor immune response (*30,31*). Non-malignant lymph nodes are known to contain PD-1 expressing immune cells (*27*). One lymph node unsuspected of malignant involvement was biopsied because it showed substantial $^{89}$Zr-pembrolizumab uptake and immunohistochemistry did indeed show high PD-1 expression in the follicles. Whether PD-1 expression in lymph nodes is necessary to obtain a response remains uncertain. In one patient, $^{89}$Zr-pembrolizumab uptake exceeded local background in benign adrenal glands. Lymphocytic infiltration of the adrenal gland has been described (*32*).

$^{89}$Zr-pembrolizumab uptake was higher in responding compared to non-responding patients, although this was not significant. Tumor tracer uptake of $^{89}$Zr-pembrolizumab increased with best tumor response category according to RECIST 1.1. Similar findings were observed for anti-

PD-L1 $^{89}$Zr-atezolizumab PET/CT (*8*). We did observe that negative lesions on $^{89}$Zr-pembrolizumab PET did not have a response to treatment, which supports our hypothesis that there is a link between uptake and response.

We were not able to find a correlation between PD-1 expression and $^{89}$Zr-pembrolizumab uptake. Heterogeneity between surgical specimens and biopsies is well known and could account for the difference in tracer uptake and PD-1 expression in a small tumor biopsy (*33,34*). This is further supported by the observation that $^{89}$Zr-pembrolizumab tracer uptake was heterogeneous both within and between tumor lesions.

**Conclusion**

This study shows that $^{89}$Zr-pembrolizumab PET/CT imaging in patients with NSCLC is safe and feasible. In this limited dataset, we found that $^{89}$Zr-pembrolizumab tracer uptake showed a non-significant correlation with response to pembrolizumab treatment. Further research is needed to investigate the value of $^{89}$Zr-pembrolizumab as standalone biomarker or as added information to tumor PD-L1 expression by immunohistochemistry.

**Financial disclosure**

This work was supported by MSD. MSD was not involved in the study design, nor in the data collection, analysis and interpretation of data, nor in the writing of this report.

**Disclaimer**

The authors have nothing to declare.

KEY POINTS

QUESTION: This study aimed (i) to investigate wheter administration of $^{89}$Zr-pembrolizumab was safe, (ii) to assess the biodistribution of $^{89}$Zr-pembrolizumab and (iii) to correlate the tracer uptake with PD-1 and PD-L1 immunohistochemistry and response to pembrolizumab treatment

PERTINENT FINDINGS: In this feasibility study, we observed that $^{89}$Zr-pembrolizumab uptake was safe, and that uptake of $^{89}$Zr-pembrolizumab was higher in patients with response (SUVpeak 11.4) than in patients without response (SUVpeak 5.7), although not statistically significant.

IMPLICATIONS FOR PATIENT CARE: Further research is needed to investigate whether $^{89}$Zr-pembrolizumab can be used as biomarker.

## References


**1.** Garon EB, Rizvi NA, Hui R, et al. Pembrolizumab for the treatment of non-small-cell lung cancer. *N Engl J Med.* 2015;372:2018-2028.

**2.** Herbst RS, Baas P, Kim DW, et al. Pembrolizumab versus docetaxel for previously treated, PD-L1-positive, advanced non-small-cell lung cancer (KEYNOTE-010): a randomised controlled trial. *Lancet.* 2016;387:1540-1550.

**3.** Mok TSK, Wu YL, Kudaba I, et al. Pembrolizumab versus chemotherapy for previously untreated, PD-L1-expressing, locally advanced or metastatic non-small-cell lung cancer (KEYNOTE-042): a randomised, open-label, controlled, phase 3 trial. *Lancet.* 2019;393:1819-1830.

**4.** Reck M, Rodriguez-Abreu D, Robinson AG, et al. Pembrolizumab versus chemotherapy for PD-L1-positive non-small-cell lung cancer. *N Engl J Med.* 2016;375:1823-1833.

**5.** Shukuya T, Carbone DP. Predictive markers for the efficacy of anti-PD-1/PD-L1 antibodies in lung cancer. *J Thorac Oncol.* 2016;11:976-988.

**6.** Van Dongen GA, Huisman MC, Boellaard R, et al. 89Zr-immuno-PET for imaging of long circulating drugs and disease targets: why, how and when to be applied? *Q J Nucl Med Mol Imaging.* 2015;59:18-38.

**7.** Niemeijer AN, Leung D, Huisman MC, et al. Whole body PD-1 and PD-L1 positron emission tomography in patients with non-small-cell lung cancer. *Nat Commun.* 2018;9:4664.

**8.** Bensch F, van der Veen EL, Lub-de Hooge MN, et al. (89)Zr-atezolizumab imaging as a non-invasive approach to assess clinical response to PD-L1 blockade in cancer. *Nat Med.* 2018;24:1852-1858.

**9.** England CG, Ehlerding EB, Hernandez R, et al. Preclinical pharmacokinetics and biodistribution studies of 89Zr-labeled pembrolizumab. *J Nucl Med.* 2017;58:162-168.

**10.** Natarajan A, Patel CB, Habte F, Gambhir SS. Dosimetry prediction for clinical translation of (64)Cu-pembrolizumab immunoPET targeting human PD-1 expression. *Sci Rep.* 2018;8:633.

**11.** Fessas P, Lee H, Ikemizu S, Janowitz T. A molecular and preclinical comparison of the PD-1-targeted T-cell checkpoint inhibitors nivolumab and pembrolizumab. *Semin Oncol.* 2017;44:136-140.

**12.** Na Z, Yeo SP, Bharath SR, et al. Structural basis for blocking PD-1-mediated immune suppression by therapeutic antibody pembrolizumab. *Cell Res.* 2017;27:147-150.

**13.** Tan S, Zhang H, Chai Y, et al. An unexpected N-terminal loop in PD-1 dominates binding by nivolumab. *Nat Commun.* 2017;8:14369.

**14.** PD-L1 IHC 22C3 pharmDx Interpretation Manual – NSCLC. October 23, 2019; https://www.agilent.com/cs/library/usermanuals/public/29158_pd-l1-ihc-22C3-pharmdx-nsclc-interpretation-manual.pdf. Accessed April 9, 2020.

**15.** Herbst RS, Soria JC, Kowanetz M, et al. Predictive correlates of response to the anti-PD-L1 antibody MPDL3280A in cancer patients. *Nature.* 2014;515:563-567.

**16.** Jauw YW, Menke-van der Houven van Oordt CW, Hoekstra OS, et al. Immuno-positron emission tomography with zirconium-89-labeled monoclonal antibodies in oncology: what can we learn from initial clinical trials? *Front Pharmacol.* 2016;7:131.

**17.** Verel I, Visser GW, Boellaard R, et al. Quantitative 89Zr immuno-PET for in vivo scouting of 90Y-labeled monoclonal antibodies in xenograft-bearing nude mice. *J Nucl Med.* 2003;44:1663-1670.

**18.** Perk LR, Vosjan MJ, Visser GW, et al. p-Isothiocyanatobenzyl-desferrioxamine: a new bifunctional chelate for facile radiolabeling of monoclonal antibodies with zirconium-89 for immuno-PET imaging. *Eur J Nucl Med Mol Imaging.* 2010;37:250-259.

**19.** Vosjan MJ, Perk LR, Visser GW, et al. Conjugation and radiolabeling of monoclonal antibodies with zirconium-89 for PET imaging using the bifunctional chelate p-isothiocyanatobenzyl-desferrioxamine. *Nat Protoc.* 2010;5:739-743.

**20.** Cohen R, Vugts DJ, Stigter-van Walsum M, Visser GW, van Dongen GA. Inert coupling of IRDye800CW and zirconium-89 to monoclonal antibodies for single- or dual-mode fluorescence and PET imaging. *Nat Protoc.* 2013;8:1010-1018.

**21.** Eisenhauer EA, Therasse P, Bogaerts J, et al. New response evaluation criteria in solid tumours: revised RECIST guideline (version 1.1). *Eur J Cancer.* 2009;45:228-247.

**22.** Frings V, van Velden FH, Velasquez LM, et al. Repeatability of metabolically active tumor volume measurements with FDG PET/CT in advanced gastrointestinal malignancies: a multicenter study. *Radiology.* 2014;273:539-548.

**23.** Boellaard R HO, Lammertsma AA. Software tools for standardized analysis of FDG whole body studies in multi-center trials [abstract]. *J Nucl Med* 2008;49:159P.

**24.** Lodge MA, Chaudhry MA, Wahl RL. Noise considerations for PET quantification using maximum and peak standardized uptake value. *J Nucl Med.* 2012;53:1041-1047.

**25.** Institute NC. Common Terminology Criteria for Adverse Events (CTCAE) version 4.0. In: v4.0 C, ed: U.S.DEPARTMENT OF HEALTH AND HUMAN SERVICES; 2009.

**26.** Pluim D, Ros W, Miedema IHC, Beijnen JH, Schellens JHM. Multiparameter flow cytometry assay for quantification of immune cell subsets, PD-1 expression levels and PD-1 receptor occupancy by nivolumab and pembrolizumab. *Cytometry A.* 2019;95:1053-1065.

**27.** Keir ME, Butte MJ, Freeman GJ, Sharpe AH. PD-1 and its ligands in tolerance and immunity. *Annu Rev Immunol.* 2008;26:677-704.

**28.** van der Veen EL, Giesen D, Pot-de Jong L, Jorritsma-Smit A, De Vries EGE, Lub-de Hooge MN. (89)Zr-pembrolizumab biodistribution is influenced by PD-1-mediated uptake in lymphoid organs. *J Immunother Cancer.* 2020;8.

**29.** Li W, Wang Y, Rubins D, et al. PET/CT imaging of (89)Zr-N-sucDf-pembrolizumab in healthy cynomolgus monkeys. *Mol Imaging Biol.* 2021;23:250-259.

**30.** Fransen MF, Schoonderwoerd M, Knopf P, et al. Tumor-draining lymph nodes are pivotal in PD-1/PD-L1 checkpoint therapy. *JCI Insight.* 2018;3.

**31.** Spitzer MH, Carmi Y, Reticker-Flynn NE, et al. Systemic immunity is required for effective cancer immunotherapy. *Cell.* 2017;168:487-502 e415.

**32.** Hayashi Y, Hiyoshi T, Takemura T, Kurashima C, Hirokawa K. Focal lymphocytic infiltration in the adrenal cortex of the elderly: immunohistological analysis of infiltrating lymphocytes. *Clin Exp Immunol.* 1989;77:101-105.

**33.** Ilie M, Long-Mira E, Bence C, et al. Comparative study of the PD-L1 status between surgically resected specimens and matched biopsies of NSCLC patients reveal major discordances: a potential issue for anti-PD-L1 therapeutic strategies. *Ann Oncol.* 2016;27:147-153.

**34.** McLaughlin J, Han G, Schalper KA, et al. Quantitative assessment of the heterogeneity of PD-L1 expression in non-small-cell lung cancer. *JAMA Oncol.* 2016;2:46-54.

**TABLE 1.**

| | |
|---|---|
| Total number of lesions determined on diagnostic CT | 216 |
| Lesions <20 mm | 140 (64.8%) |
| Lesions ≥20 mm | 72 (33.3%) |
| Measurement unreliable* | 4 (1.8%) |
| Lesions visible on PET/CT scan | 62 (28.7%) |
| Lesions <20 mm | 26 (18.6%) |
| Lesions ≥20 mm | 34 (47.2%) |
| Measurement unreliable* | 2 |
| Lesions without uptake >20 mm | 38 |
| Brain | 2 |
| Lymph node | 7 |
| Lung | 2 |
| Bone | 12 |
| Liver | 12 |
| Adrenal gland | 2 |
| Soft tissue | 1 |

**Lesions on diagnostic CT and $^{89}$Zr-pembrolizumab PET.** * Measurement of these lesions were unreliable due to atelectasis.

**FIGURES**

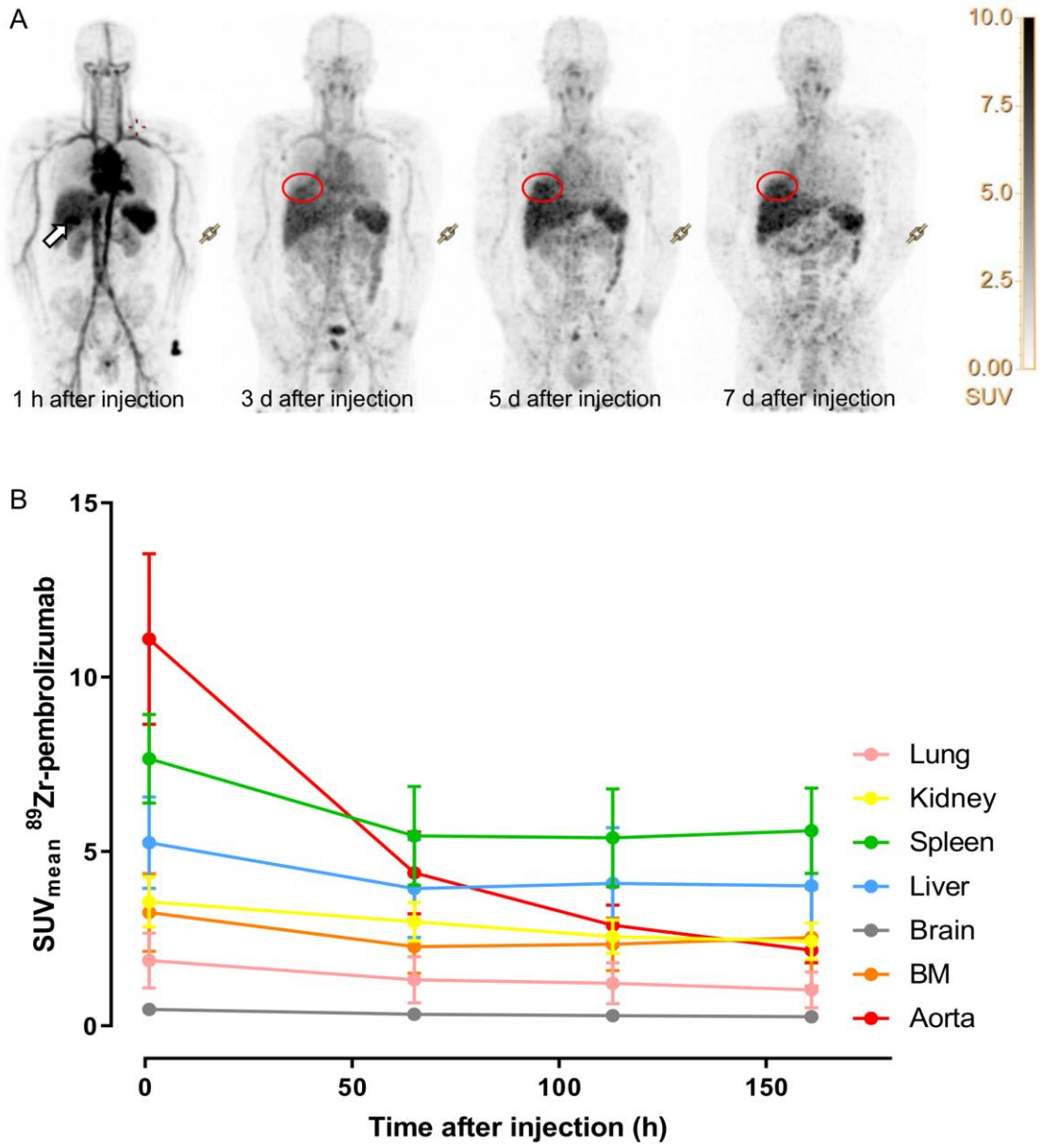


**FIGURE 1**

Biodistribution of $^{89}$Zr-pembrolizumab. A Maximum Intensity Projection image of patient 1. White arrow indicates the gall bladder. Red circle indicates the primary tumor. B Tracer uptake per time point, measured as mean $SUV_{mean}$; measured for the first 3 patients on 1.1±0.3 (SD) h post-injection (p.i.), 65.8±0.3 h p.i., 113.2±0.7 h p.i. and 161.4±0.81h p.i..

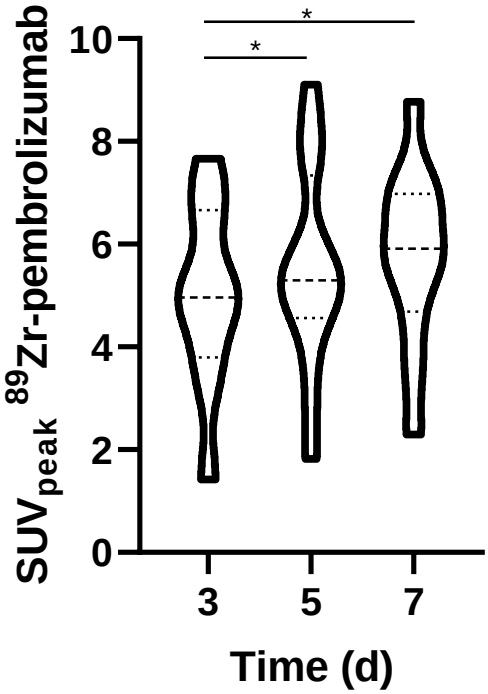


**FIGURE 2**

Median SUVpeak of all lesions for all patients.

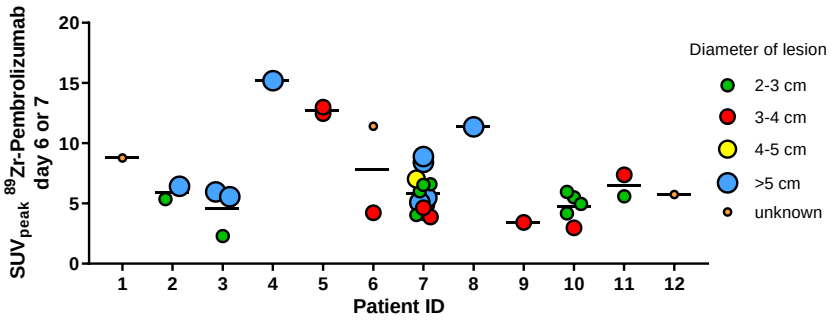


**FIGURE 3**

$^{89}$Zr-pembrolizumab tumor uptake for all patients per delineated tumor.

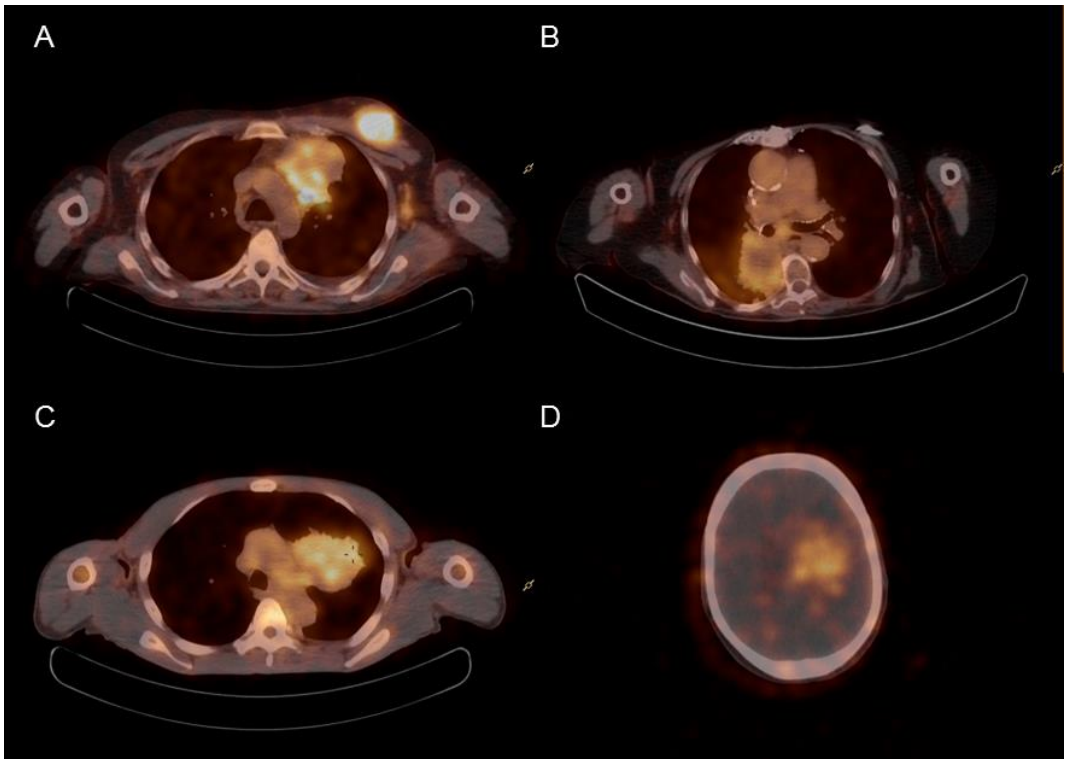


**FIGURE 4**

**$^{89}$Zr-pembrolizumab uptake patterns.**

A Heterogeneous uptake in a paracardial mass and homogeneous uptake in a soft tissue mass in the left breast. B Rim uptake. C Heterogeneous uptake. D Uptake in a brain metastasis.

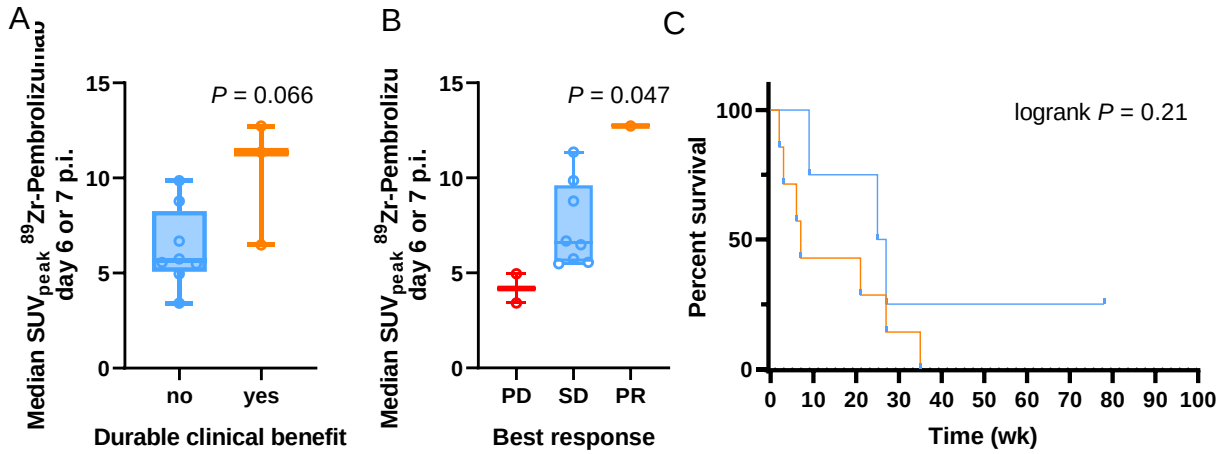


**FIGURE 5**

**Relation between tracer uptake and response**

A Median tracer uptake of all lesions >20 mm for responders and non-responders. B Median tracer uptake per best RECIST response category. C Progression free survival curve according to the median SUVpeak (blue, above median SUVpeak 6.7; orange, below median SUVpeak).

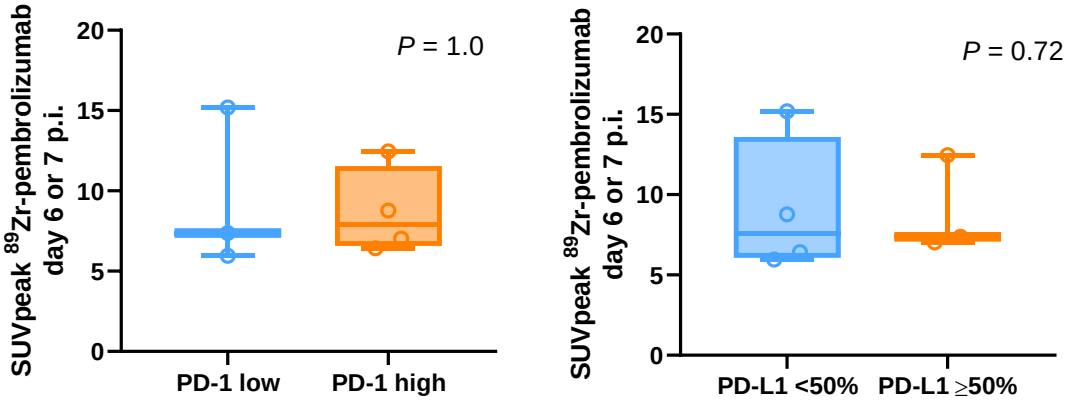


**FIGURE 6**

**Relation between tracer uptake and immunohistochemistry.**

A Correlation between SUVpeak and PD-1 expression of biopsied lesion. B Correlation between SUVpeak and PD-L1 expression of biopsied lesion.

Graphical abstract

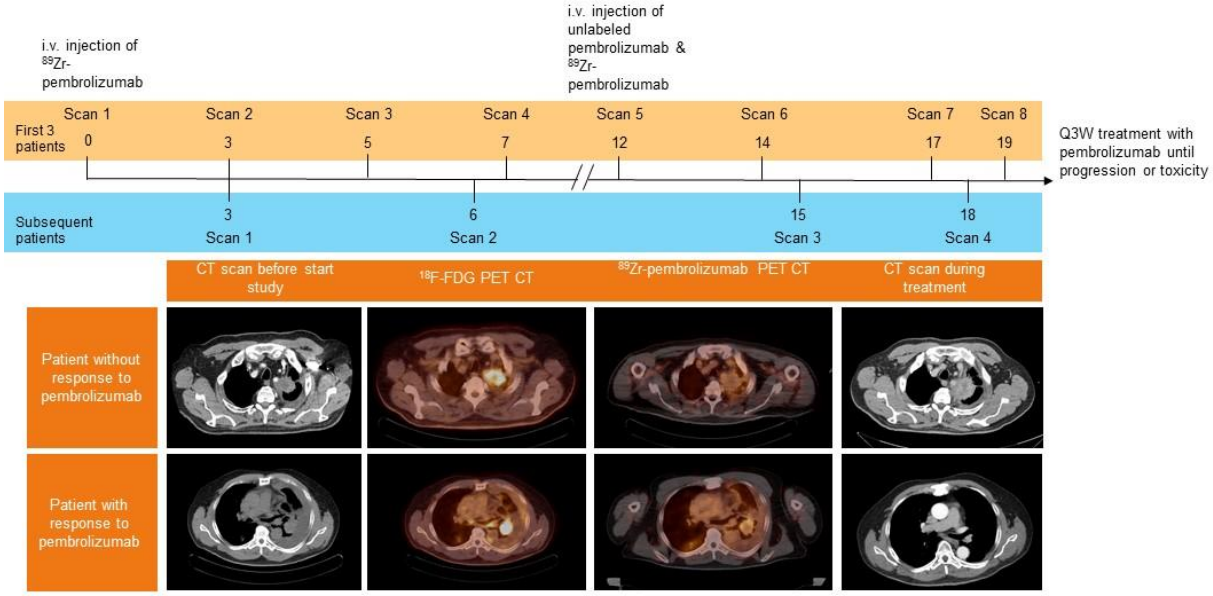

*SUPPLEMENTARY MATERIAL*

*Production of $^{89}$Zr -Pembrolizumab*

In short, 5 mg pembrolizumab (0.2 mL, 25 mg/mL) was mixed with 770 µL 0.9% NaCl and the pH of the solution was adjusted to 8.9-9.1 with 0.1 M $Na_2CO_3$. Next, this solution was added to 20 µL of 5 mM (3 equivalents) NCS-Bz-DFO in DMSO (Macrocyclics, Boston, USA) and incubated for 30 min at 37˚C at 550 rpm in a thermomixer. After purification by size exclusion chromatography (PD10, GE Healthcare) to remove unreacted DFO-Bz-NCS, the product, DFO-pembrolizumab, was radiolabelled with zirconium-89 in a 2 mL reaction. The reaction mixture consisting of 200 µL 1M oxalic acid (containing the required amount of $^{89}$Zr), 90 µL 2M $Na_2CO_3$, 1 mL 0.5 M Hepes and 0.71 mL DFO-Pembrolizumab (~1.7 mg) was reacted for 60 minutes at room temperature while slowly shaken. The product was isolated by size exclusion chromatography using a PD10 column. The product was eluted in 50 mM NaOAc + 200 mM Sucrose pH 5.5 ± 0.3 and formulated to arrive at an injection dose of 37 MBq – 2 mg – 20 mL [$^{89}$Zr]Zr-Pembrolizumab. The following quality controls were performed and met the pre-set specifications. pH: 5.7 ± 0.2; radiochemical purity: 99.1 ± 0.8% (spin filter) and 99.8 ± 0.9 % (SE-HPLC); protein integrity: 100.0 ± 0.1 %; immune reactive fraction (binding assay): 89.6 ± 4.4 %; endotoxin content: <0.2 EU/mL [1]. Size exclusion HPLC was performed using a superdex increase 200 10/30 GL size exclusion column (GE healthcare Life sciences) including a guard column using a mixture of 0.05 M sodium phosphate, 0.15 M sodium chloride (pH 6.8) and 0.01 M $NaN_3$ as the eluent at a flow rate of 0.5 mL/min. Sterility of each $^{89}$Zr-pembrolizumab batch was assured by performing a media fill immediately after final filter sterilisation of each batch of [$^{89}$Zr]Zr-pembrolizumab.

References

1. Vugts DJ, Klaver C, Sewing C, et al: Comparison of the octadentate bifunctional chelator DFO*-pPhe-NCS and the clinically used hexadentate bifunctional chelator DFO-pPhe-NCS for (89)Zr-immuno-PET. Eur J Nucl Med Mol Imaging 44:286-295, 2017

**SUPPLEMENTARY TABLE 1.**

| **Baseline characteristics** | **N (%)** | **First line** | **Second/third line** | ***P*-value** |
|---|---|---|---|---|
| Median age, years | 67.0 | 67.0 | 66.5 | 0.93 |
| Sex | | | | 0.93 |
| Male | 7 (58.3) | 3 (60.0) | 4 (57.1) | |
| Female | 5 (41.7) | 2 (40.0) | 3 (42.9) | |
| WHO performance status | | | | 0.69 |
| 0 | 4 (33.3) | 2 (40.0) | 2 (28.6) | |
| 1 | 8 (66.7) | 3 (60.0) | 5 (71.4) | |
| Tumor PD-L1 expression | | | | 0.020 |
| <1 % | 4 (33.3) | 0 | 4 (57.1) | |
| 1-49 % | 3 (25.0) | 1 (20.0) | 2 (28.6) | |
| >50% | 5 (41.7) | 4 (80.0) | 1 (14.3) | |
| PD-1 expression | | | | 0.015 |
| IC0 | 3 (25.0) | 0 | 3 (42.9) | |
| IC1 | 4 (33.3) | 1 (20.0) | 3 (42.9) | |
| IC2 | 2 (16.7) | 1 (20.0) | 1 (14.3) | |
| IC3 | 3 (25.0) | 3 (60.0) | 0 | |
| Number of previous anticancer regimens | | | | 0.002 |
| 0 | 5 (41.7) | 5 (100) | 0 | |
| 1 | 5 (41.7) | 0 | 5 (71.4) | |
| 2 | 2 (16.7) | 0 | 2 (28.6) | |

**Patient baseline characteristics.** WHO world health organization; PD-L1 programmed death-ligand 1; PD-1 programmed cell death protein 1; IC immune score according to SP142

**SUPPLEMENTARY TABLE 2.**

| | **Adverse events** |
|---|---|
| **Patient 1** | Fatigue grade I<br>Anorexia grade I<br>Atelectasis grade II |
| **Patient 2** | Fatigue grade I<br>Anorexia grade I<br>Dyspnea grade II |
| **Patient 3** | Fatigue grade II<br>Anorexia grade II<br>Dizziness grade I<br>Constipation grade II |
| **Patient 4** | Dyspnea grade I |
| **Patient 5** | None |
| **Patient 6** | None |
| **Patient 7** | Anemia grade III |
| **Patient 8** | Cough grade I<br>Productive cough grade II |
| **Patient 9** | Non cardiac chest pain grade II |
| **Patient 10** | Fatigue grade I |
| **Patient 11** | None |
| **Patient 12** | Myalgia grade III |

**Adverse events per patient.**

**SUPPLEMENTARY TABLE 3.**

| | | First imaging acquisition | | | Second imaging acquisition | | |
|---|---|---|---|---|---|---|---|
| | | **Day 3** | **Day 5** | **Day 6 or 7** | **Day 14 or 15** | **Day 17** | **Day 18 or 19** |
| **Patient 1** | primary tumor | 0.11 | 0.13 | 0.13 | 0.13 | 0.16 | 0.23 |
| **Patient 2** | primary tumor | 0.05 | 0.05 | 0.07 | BLQ | 0.07 | 0.07 |
| | lymph node | 0.06 | 0.06 | 0.06 | BLQ | BLQ | BLQ |
| **Patient 3** | primary tumor | 0.08 | 0.08 | 0.09 | NP | 0.07 | 0.07 |
| | bone metastasis | 0.08 | 0.08 | 0.10 | NP | 0.07 | 0.07 |
| | bone metastasis | 0.02 | 0.03 | 0.04 | NP | 0.04 | 0.04 |
| **Patient 4** | primary tumor | 0.18 | NP | 0.21 | 0.14 | NP | 0.20 |
| **Patient 5** | primary tumor | 0.13 | NP | 0.14 | 0.14 | NP | 0.17 |
| | lung metastasis | 0.12 | NP | 0.14 | 0.15 | NP | 0.16 |
| **Patient 6** | brain metastasis | 0.05 | NP | 0.07 | NP | NP | NP |
| | lymph node | 0.13 | NP | 0.12 | NP | NP | NP |
| **Patient 7** | primary tumor | 0.10 | NP | 0.08 | 0.08 | NP | NP |
| | bone metastasis | 0.05 | NP | 0.07 | 0.04 | NP | NP |
| | bone metastasis | 0.08 | NP | 0.08 | 0.05 | NP | NP |
| | lymph node | 0.08 | NP | 0.06 | 0.06 | NP | NP |
| | soft tissue | 0.16 | NP | 0.11 | 0.06 | NP | NP |
| | bone metastasis | 0.06 | NP | 0.06 | 0.05 | NP | NP |
| | soft tissue | 0.09 | NP | 0.07 | 0.05 | NP | NP |
| | soft tissue | 0.09 | NP | 0.06 | 0.05 | NP | NP |
| | bone metastasis | 0.08 | NP | 0.09 | 0.05 | NP | NP |
| | bone metastasis | 0.09 | NP | 0.10 | 0.05 | NP | NP |
| | bone metastasis | 0.05 | NP | 0.10 | 0.05 | NP | NP |
| | soft tissue | 0.15 | NP | 0.13 | 0.07 | NP | NP |
| | soft tissue | 0.14 | NP | 0.13 | 0.07 | NP | NP |
| **Patient 8** | primary tumor | 0.18 | NP | 0.22 | 0.24 | NP | 0.27 |
| **Patient 9** | primary tumor | 0.05 | NP | 0.06 | BLQ | NP | 0.07 |
| **Patient 10** | brain metastasis | 0.03 | NP | 0.05 | 0.05 | NP | 0.06 |
| | bone metastasis | 0.06 | NP | 0.08 | BLQ | NP | BLQ |
| | bone metastasis | 0.08 | NP | 0.09 | BLQ | NP | BLQ |
| | bone metastasis | 0.04 | NP | 0.07 | BLQ | NP | BLQ |
| | bone metastasis | 0.08 | NP | 0.09 | BLQ | NP | BLQ |
| **Patient 11** | primary tumor | 0.08 | NP | 0.08 | 0.11 | NP | 0.14 |
| | lymph node | 0.10 | NP | 0.11 | BLQ | NP | BLQ |
| **Patient 12** | soft tissue | BLQ | NP | 0.08 | BLQ | NP | BLQ |

**%ID/gr for all lesions and time points after first and second 89Zr-pembrolizumab injection.**
BLQ below quantification limit; NP not performed.

**SUPPLEMENTARY TABLE 4.**

| **Patient** | **Number of brain metastases ≤10 mm** | **Number of brain metastases >10 mm but ≤20 mm** | **Number of brain metastases >20 mm (number)** | **Number of irradiated brain metastases** | **Number of visible brain metastases on $^{89}$Zr-pembrolizumab** |
|---|---|---|---|---|---|
| *Patient 1* | 5 | | | 5 | 0 |
| *Patient 2* | 8 | 2 | 2 | 12 | 0 |
| *Patient 6* | | | 1 | 1 | 1 |
| *Patient 10* | 13 | 6 | 1 | 0 | 2 |

**Brain metastases.** Information of all brain metastases in participants and visualization on $^{89}$Zr-pembrolizumab PET/CT.

**SUPPLEMENTARY TABLE 5.**

| Patient | PD-L1 expression (%) | PD-1 expression | SUVpeak day 6/7 |
|---|---|---|---|
| 1 | 0 | IC2 | 8.8 |
| 2 | 20 | IC2 | 6.4 |
| 3 | 1 | IC0 | 6.0 |
| 4 | 0 | IC1 | 15.2 |
| 5 | 80 | IC3 | 12.5 |
| 6 | 0 | IC0 | BLQ |
| 7 | 75 | IC3 | 7.0 |
| 8 | 90 | IC3 | BLQ |
| 9 | 0 | IC0 | BLQ |
| 10 | 30 | IC1 | BLQ |
| 11 | 60 | IC1 | 7.4 |
| 12 | 60 | IC1 | BLQ |

**SUVpeak and immunohistochemistry.** Characteristics of each biopsied lesion including PD-L1 expression, PD-1 expression and SUVpeak on day 6 or 7.
PD-L1 programmed death-ligand 1; PD-1 programmed cell death protein 1; SUV standardized uptake value; BLQ below limit of quantification.

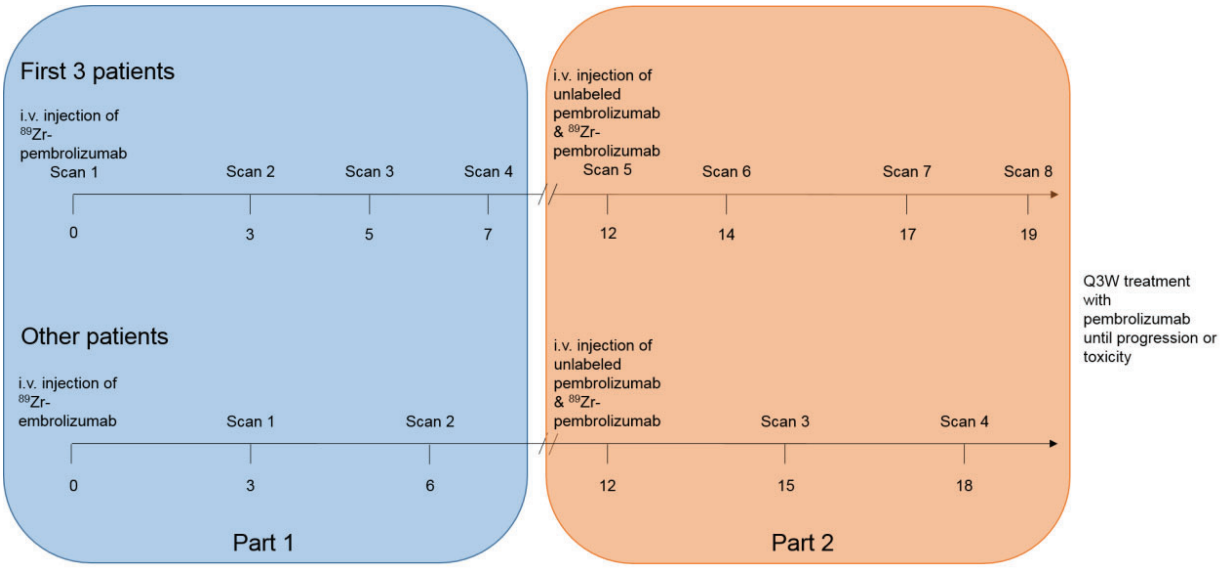


**Supplementary Figure 1**

**Study overview.** $^{89}$Zr-pembrolizumab (37 MBq ±10%, 2 mg pembrolizumab) was intravenously (IV) injected on day 0. Static whole body PET/CT scans were performed 1 hour, and 3, 5 and 7 days post injection (p.i.) for the first 3 patients, while all other patients were scanned on day 3 and 6 p.i.. On day 12, patients received an infusion with 200 mg unlabeled pembrolizumab, within two hours followed by a second $^{89}$Zr-pembrolizumab injection, to maximize the chance of representing therapeutic tumor targeting.

*i.v.* intravenous *$^{89}$Zr* labeled pembrolizumab *Q3W* every three weeks

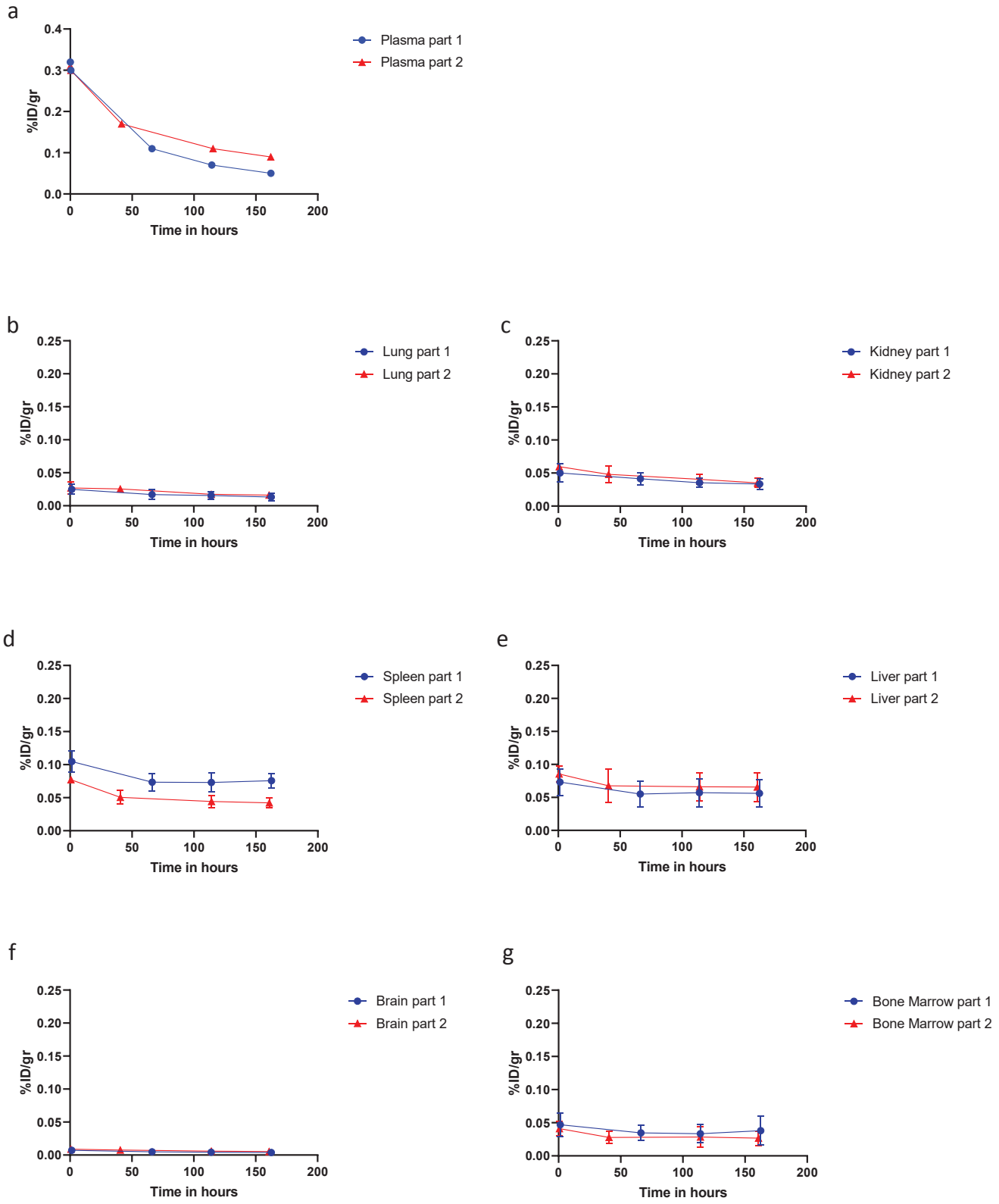


**Supplementary Figure 2**

Activity concentrations in first and second imaging acquisition in plasma and in organs.

*%ID/gr* percentage injected dose per gram tissue

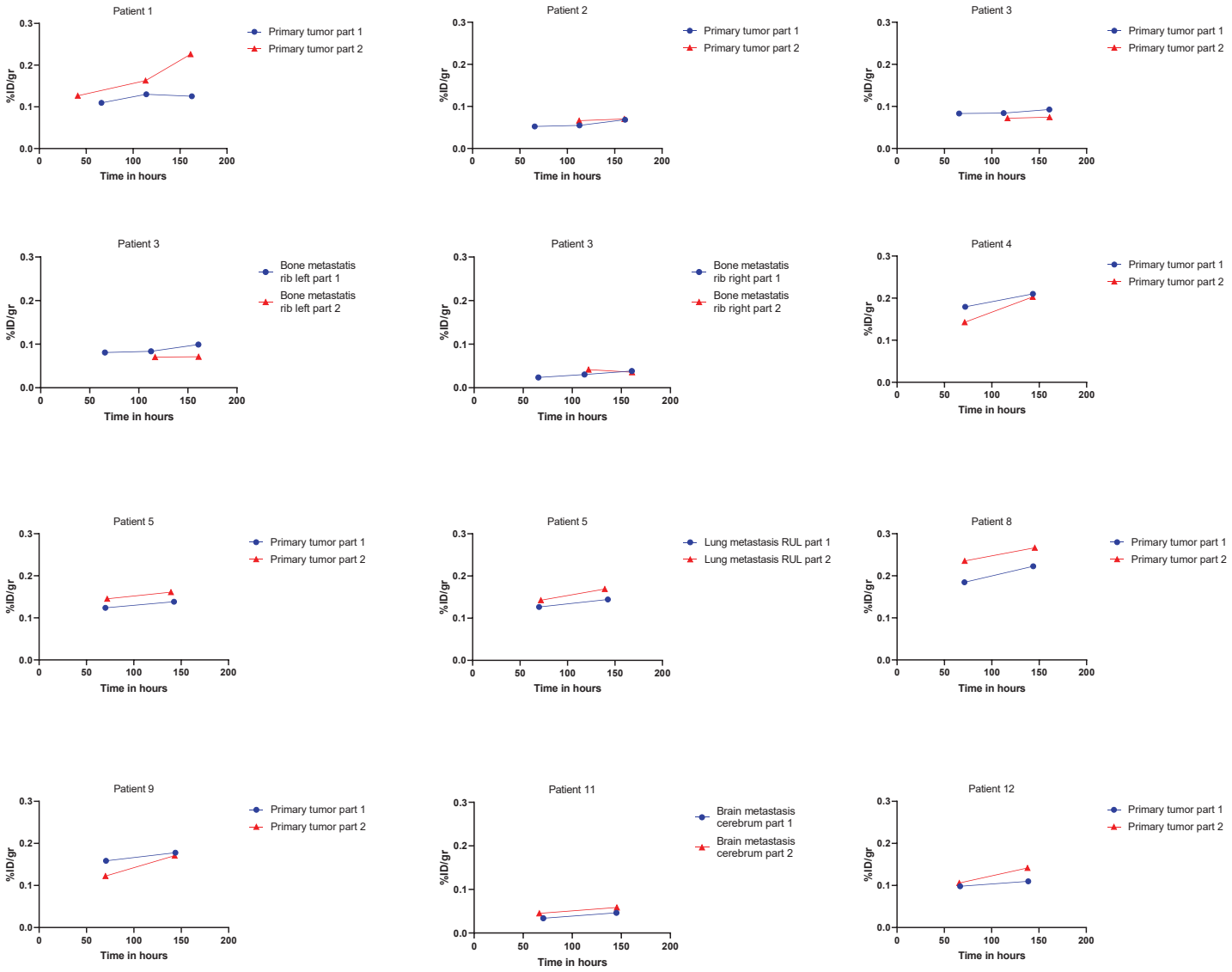


**Supplementary Figure 3**

Activity concentrations (in %ID/gr) in first and second imaging acquisition in tumor.

*%ID/gr* percentage injected dose per gram tissue

a

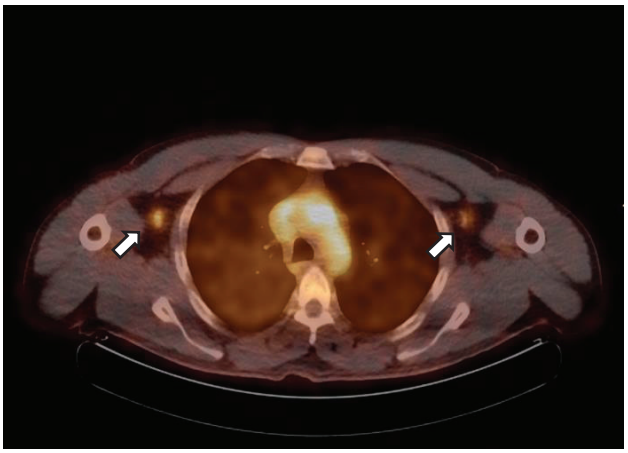

b

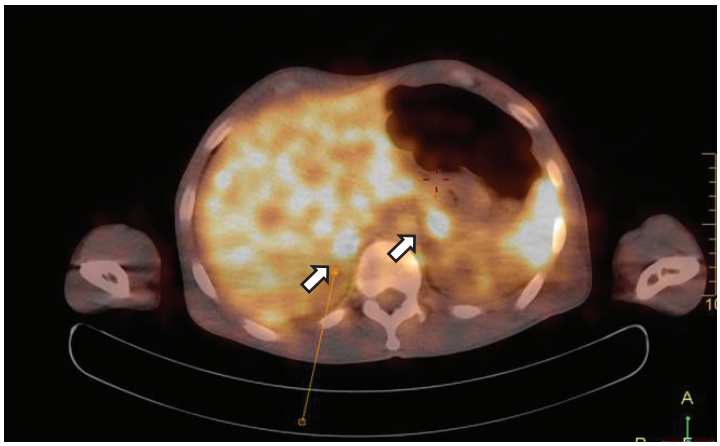


**Supplementary Figure 4**

Non-malignant tissues (axillary lymph nodes, a; adrenal gland, b) showed uptake of $^{89}$Zr-pembrolizumab.